

- [11] In this case, the cyclopentadiene **6** could not be detected in the crude reaction mixture before H₂O/HOAc (6:1) had been added. Addition of aqueous hydrochloric acid gave **6** in much lower yield (22%), addition of pure water gave no **6** at all.
- [12] Crystal structure analyses: **13** (C₃₄H₄₂Fe): *Z* = 4, *M*_r = 506.56, crystal dimensions: 0.50 × 0.40 × 0.40 mm, monoclinic, space group *P*2₁, *a* = 876.8(2), *b* = 3494.8(7), *c* = 897.2(2) pm, *β* = 102.34(3)°, *V* = 2.6859(9) nm³, *ρ*_{calcd} = 1.253 Mg m⁻³, *F*(000) = 1088, *λ* = 71.073 pm, *T* = 133(2) K, *μ*(MoK_α) = 0.582 mm⁻¹, 2.32° ≤ 2*θ* ≤ 25.02°; out of 33365 collected reflections, 9498 are independent and were used for structure refinement of 632 parameters. The *R* values are *R*₁ = 0.0370 (*I* > 2*σ*(*I*)) and *wR*₂ = 0.0716 (all data); min./max. residual electron density: -345/189 e nm⁻³. **14** (C₄₀H₅₀Fe): *Z* = 1, *M*_r = 586.65, crystal dimensions: 0.60 × 0.40 × 0.50 mm, triclinic, space group *P*1̄, *a* = 911.2(2), *b* = 982.6(2), *c* = 1043.6(2) pm, *α* = 117.56(1)°, *β* = 107.35(1)°, *γ* = 90.38(1)°, *V* = 0.7790(2) nm³, *ρ*_{calcd} = 1.251 Mg m⁻³, *F*(000) = 316, *λ* = 71.073 pm, *T* = 133(2) K, *μ*(MoK_α) = 0.511 mm⁻¹, 2.38° ≤ 2*θ* ≤ 24.74°; out of 6373 collected reflections, 2606 are independent and were used for structure refinement of 175 parameters. The *R* values are *R*₁ = 0.0666 (*I* > 2*σ*(*I*)) and *wR*₂ = 0.1926 (all data); min./max. residual electron density: -581/1142 e nm⁻³. CCDC-172568 (**13**) and CCDC-172569 (**14**) contain the supplementary crystallographic data for this paper. These data can be obtained free of charge via www.ccdc.cam.ac.uk/conts/retrieving.html (or from the Cambridge Crystallographic Data Centre, 12, Union Road, Cambridge CB2 1EZ, UK; fax: (+44) 1223-336-033; or deposit@ccdc.cam.ac.uk).
- [13] N. A. Ogorodnikova, D. N. Kravtsov, *Polyhedron* **1985**, *4*, 311–316.
- [14] J. L. Robbins, N. Edelstein, B. Spencer, J. C. Smart, *J. Am. Chem. Soc.* **1982**, *104*, 1882–1893.
- [15] H. Sitzmann, *J. Organomet. Chem.* **1988**, *354*, 203–214.
- [16] H. Sitzmann, *Z. Naturforsch. B* **1989**, *44*, 1293–1297.
- [17] P. S. Nielsen, R. S. Hansen, H. J. Jakobsen, *J. Organomet. Chem.* **1976**, *114*, 145–155.
- [18] a) H. Sitzmann, R. Boese, *Angew. Chem.* **1991**, *101*, 1027–1029; *Angew. Chem. Int. Ed. Engl.* **1991**, *30*, 971–973; b) H. Sitzmann, H. Bock, R. Boese, T. Dezember, Z. Havlas, W. Kaim, M. Moscherosch, L. Zanathy, *J. Am. Chem. Soc.* **1993**, *115*, 12003–12009.
- [19] D. P. Freyberg, J. L. Robbins, K. N. Raymond, J. C. Smart, *J. Am. Chem. Soc.* **1979**, *101*, 892–897.
- [20] An attempt to prepare pentamethylcyclopentadiene from 2-butyne and ethyl acetate by applying the newly developed protocol for pentacyclopentadiene (**6**) was not met with success. Pentamethylcyclopentadiene has, however, successfully been prepared from 2-bromo-2-butene and ethyl acetate via the butenyllithium derivative and pentamethylpentadienol. See: R. S. Threlkel, J. E. Bercaw, *J. Organomet. Chem.* **1977**, *136*, 1–5.

Spinel Sialons**

Marcus Schwarz,* Andreas Zerr, Edwin Kroke,*
Gerhard Miehe, I-Wei Chen, Martin Heck,
Brunhilde Thybusch, Brent T. Poe, and Ralf Riedel

In the system Si–Al–O–N and related multinary systems a large variety of crystalline and vitreous phases is known. These so called sialons are of technological importance, especially for applications as structural ceramics.^[1] The term “classical sialons” refers to the solid solutions of Al₂O₃, (AlN), and Si₃N₄, known as *β*-sialons because of their close structural relationship to *β*-Si₃N₄.^[2] By analogy, *α*-sialons can be derived from *α*-Si₃N₄, but they also incorporate metal ions such as Li, Ca, and Y and most rare earth metals.^[1,2] These Si–Al–O–N systems have been extensively studied. Haviar et al. reported their behavior at high temperature (up to 1800 °C) and high pressure (up to 6 GPa).^[3]

Here we report the synthesis and structure determination of a high-pressure sialon phase with spinel structure (space group *Fd3m*) by conversion of *β*-Si₂AlON₃ at 13 GPa/1800 °C. Its hardness of 27.5 GPa significantly exceeds those of *β*- and *α*-sialons.

This work extends the recent discovery of binary spinel nitrides *γ*-E₃N₄ (E = Si, Ge, Sn),^[4] in which both octahedral and tetrahedral lattice sites are occupied by cations with a

[*] Dipl.-Ing. M. Schwarz, Dr. E. Kroke,^[+] Dr. A. Zerr,
Prof. Dr. R. Riedel
Fachgebiet Disperse Feststoffe
Fachbereich Material- und Geowissenschaften
Technische Universität Darmstadt
Petersenstraße 23, 64287 Darmstadt (Germany)
Fax: (+49) 6151-166346
E-mail: mrschw@tu-darmstadt.de
kroke@tu-darmstadt.de

Dr. G. Miehe
Fachgebiet Strukturforschung
Fachbereich Material- und Geowissenschaften
Technische Universität Darmstadt (Germany)

Dr. M. Heck, B. Thybusch
Fachgebiet Chemische Analytik
Fachbereich Material- und Geowissenschaften
Technische Universität Darmstadt (Germany)

Dr. B. T. Poe
Bayerisches Geoinstitut
Universität Bayreuth
95440 Bayreuth (Germany)

Prof. Dr. I-W. Chen
University of Pennsylvania
3231 Walnut Street, 424 LRSM
Philadelphia, PA 19104-6272 (USA)

[+] Current address: Materials Department
University of California, Santa Barbara
Santa Barbara, CA 93436 (USA)
Fax: (+1) 805-893-8486

[**] We gratefully acknowledge the synthesis of *β*-sialon starting material by M. Zenotckine and the fruitful conversation with James W. McCauley concerning the existence of *γ*-Al₂O₃N. The department of high-pressure/mineral physics, Max-Planck-Institut für Chemie, Mainz, is acknowledged for providing technical support. We are further grateful for the financial support of this work provided by the Deutsche Forschungsgemeinschaft and the Fonds der Chemischen Industrie. E.K. thanks the Alexander von Humboldt Foundation for granting a Lynen fellowship.

formal charge of +4 (4-4 spinels). It was motivated by the observation that β -sialon can be formally derived from β - Si_3N_4 by substituting SiN pairs by AlO. Thus, the composition follows the formula $\text{Si}_{3-x}\text{Al}_x\text{O}_x\text{N}_{4-x}$,^[5] whereby the β - Si_3N_4 structure is known to exist up to $x_{\text{max}} \approx 2.1$. The composition $\text{Al}_3\text{O}_3\text{N}$, corresponding to full substitution ($x=3$), is said to have spinel structure but in fact has not been observed to the present day.^[6] However, at even higher degrees of AlO insertion ($4.2 \leq x \leq 4.7$; $\text{Al}_{[3+(x-3)/3]}\text{O}_x\text{N}_{[1-(x-3)/3]}$), stable spinels containing (cation-vacancy-type) defects, the so called γ -alons, are known.^[7] Their existence and the discovery of the spinel γ - Si_3N_4 ($\equiv c\text{-Si}_3\text{N}_4$)^[4a, 8] prompted us to investigate the possible formation of γ -sialon with the composition $\text{Si}_{3-x}\text{Al}_x\text{O}_x\text{N}_{4-x}$ at high pressure.

For our experiments we chose a single-phase β -sialon starting material with $x=1$ (Si_2AlON_3). The composition was verified by X-ray powder diffraction (XRD), by using the known dependence of lattice constants on x ^[9], and electron-probe microanalysis (EPMA). Scanning electron microscopy (SEM) revealed grain sizes of 1–2 μm . High-pressure conversion was carried out in a 6-8 type multi-anvil (MA) apparatus.^[8, 10] The applied pressure of 13 GPa was slightly above that at which γ - Si_3N_4 was synthesized.^[8]

While the color of the starting material was white, the recovered sialon had a dark gray, opaque appearance. SEM studies of fractured surfaces of the starting sialon showed equiaxed grains, similar to kelvin polyhedra, which had changed into more irregular morphologies in the recovered sample. The grain size, however, had decreased to less than 1 μm . A smaller grain size is commonly observed after phase transformations. Within the resolution of SEM, no pores were visible on the ground surface. The chemical composition of the sample, determined by EPMA, was identical to that of the starting sialon and homogeneous within the investigated area (100 \times 100 μm).

The spinel structure was verified by XRD and high-resolution transmission electron microscopy (HR-TEM). Initially, a piece of the recovered sample was ground in an agate mortar. However, we found this caused considerable wear of the mortar (evidenced by surface roughening) because of the high hardness of the material. The resulting XRD pattern (data set I) showed the presence of α -quartz that could be traced to debris from the mortar. A volume fraction of quartz as high as 20% was determined in a Rietveld refinement. Using the quartz as an internal standard, we determined a lattice parameter $a_0^{\text{I}} = 7.823$ Å. In a second approach, a piece of the recovered material was mounted in a capillary on a Gandolfi camera. The diffraction pattern of this sample, with the background subtracted (data set II), is shown in Figure 1, along with its Rietveld difference plot. All reflections can be assigned to a spinel structure. This proves the presence of a single-phase material, hereafter named γ - Si_2AlON_3 .

The geometry of the Gandolfi method causes the lattice constant a_0^{II} to critically depend on the exact value of the distance between the sample and the X-ray film or imaging plate. We therefore consider a_0^{I} derived from data set I using quartz as a standard to be more precise. In contrast, the recorded intensities are not affected, and Rietveld refinement

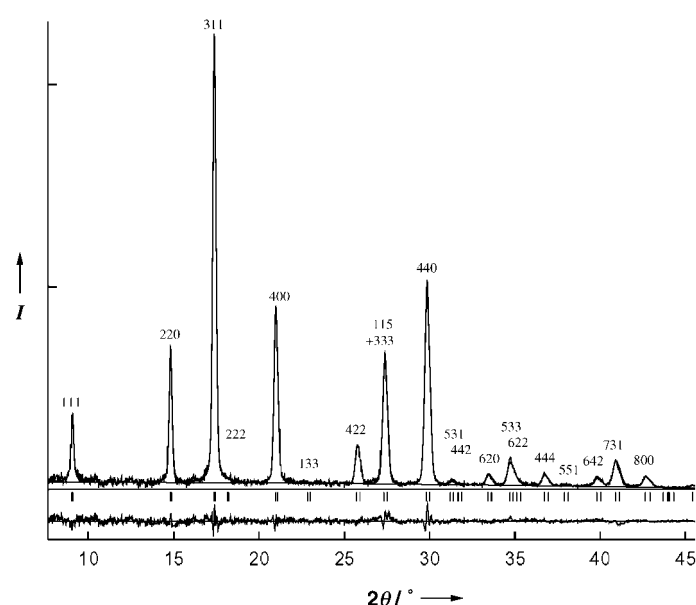


Figure 1. Powder X-ray diffractogram of γ - Si_2AlON_3 (background subtracted) and the corresponding Rietveld difference plot. The line positions are indicated with respect to $\text{MoK}_{\alpha 1}$ and $\text{MoK}_{\alpha 2}$ radiation, respectively.

using data set II yielded better GOF and R_{Bragg} than of data set I. The crystallographic data for both data sets are listed in Table 1. Table 2 lists the atomic coordinates from the respective refinements.

In the spinel structure, the anions are located at (x,x,x) (Wyckoff position 32e), and $x \equiv x_{\text{N/O}}$ is the only free param-

Table 1. Crystallographic data for γ - Si_2AlON_3 .

γ - Si_2AlON_3	data set I	data set II
M_r [g mol ⁻¹]	141.17	
Space group	$Fd\bar{3}m$ (no. 227)	
Radiation, λ [Å]	$\text{CuK}_{\alpha 1}$, 1.54056	MoK_{α} , 0.7107
Lattice param. a_0 [Å]	7.8234(3)	7.7994(7) ^[a]
V [Å ³]	478.76	474.44 ^[a]
Z	8	8
ρ_{calcd} [g cm ⁻³]	3.92	3.95 ^[a]
Profile range	$18.0 \leq 2\theta \leq 87.9^\circ$	$7.6 \leq 2\theta \leq 45.9^\circ$
Step size	$2\theta = 0.02^\circ$	$2\theta = 0.02^\circ$
Varied parameters	37 ^[b]	21
Profile function	pseudo-Voigt	pseudo-Voigt
R values [%]	$R = 4.80$ $R_w = 6.36$ $R_{\text{Bragg}} = 6.99$ GOF: 2.05	$R = 8.54$ $R_w = 13.61$ $R_{\text{Bragg}} = 4.56$ GOF: 1.55

[a] Value of a_0^{II} not corrected for uncertainties in the sample-to-imaging-plate distance. [b] Including parameters for quartz.

Table 2. Atomic coordinates for γ - Si_2AlON_3 .

Data set	Atom	Wyckoff position	x	y	z	B_{iso}
I	Al/Si	8a	1/8	1/8	1/8	1.40(6)
	Si/Al	16d	1/2	1/2	1/2	–1.8(1) ^[b]
	N/O ^[a]	32e	0.2591(2)	0.2591(2)	0.2591(2)	5.2(1) ^[b]
II	Al/Si	8a	1/8	1/8	1/8	1.23(8)
	Si/Al	16d	1/2	1/2	1/2	1.3(1) ^[b]
	N/O ^[a]	32e	0.2550(4)	0.2550(4)	0.2550(4)	2.4(1) ^[b]

[a] For N/O at 32e: $x = y = z = x_{\text{N/O}}$. [b] Isotropic equivalents.

eter. In a spinel with an ideal fcc anion lattice, $x_{\text{N/O}}$ is equal to $1/4$.^[11] A deviation from this value leads to a distorted environment of the octahedral cation sites. The parameter $x_{\text{N/O}}$ is often referred to as “spinel parameter” u and is used to compare anion environments, as shown below.^[12, 13] In the present case a value of $x_{\text{N/O}}^{\text{II}} = 0.255$ ($R_{\text{Bragg}} = 4.56$) was determined from data set II, while data set I yielded $x_{\text{N/O}}^{\text{I}} = 0.259$ ($R_{\text{Bragg}} = 6.99$). From a_0^{I} and $x_{\text{N/O}}^{\text{I}}$, we calculated the average bond lengths between the tetrahedrally and octahedrally coordinated cations and their nearest anionic neighbors, hereafter called $\langle \text{tet-N/O} \rangle$ and $\langle \text{oct-N/O} \rangle$, respectively (Table 2).^[14] The values for $\gamma\text{-Si}_3\text{N}_4$, $\gamma\text{-Si}_2\text{AlON}_3$, and three oxygen-rich γ -alons are listed in Table 3. A comparison between $\gamma\text{-Si}_3\text{N}_4$ and $\gamma\text{-Si}_2\text{AlON}_3$ reveals that $\langle \text{tet-N/O} \rangle$ has decreased from 1.805 to 1.762 Å, while $\langle \text{oct-N/O} \rangle$ has increased from 1.863 to 1.918 Å. The latter change is apparently responsible for the lattice expansion from 7.74 to 7.82 Å. Further insertion of AlO probably causes $\langle \text{tet-N/O} \rangle$ to lengthen, since the (ambient-pressure) γ -alons reported in [12] have $\langle \text{tet-N/O} \rangle$ values of around 1.8 Å. This phenomenon can be explained by assuming preferences of the Si and Al atoms for tetrahedral and octahedral sites, respectively. First, we note that the $\text{Si}_{\text{tet}}\text{-N}$ bond in $\gamma\text{-Si}_3\text{N}_4$ is longer than that in both α - and $\beta\text{-Si}_3\text{N}_4$ to match the larger SiN_6 octahedra in $\gamma\text{-Si}_3\text{N}_4$.^[8, 15] In $\gamma\text{-Si}_2\text{AlON}_3$, on the other hand, some Si_{oct} are now replaced by Al_{oct} , and this would allow the Si-centered tetrahedra to shrink towards their “normal” size. In γ -alons, however, both octahedral and tetrahedral sites are occupied by the bulkier Al ion, and hence the tetrahedral bond length increases again. This explanation is consistent with the observed variations of bond length and the expectations from the consideration of cation size.

The above discussion suggests that $\gamma\text{-Si}_2\text{AlON}_3$ is an inverse spinel in which the lower valent cation preferentially occupies the sites with higher coordination numbers. (The opposite case is referred to as a normal spinel.) This is further supported by a comparison with the structural parameters of known spinels: The anion parameters u of 2-3 and 4-2 spinels (here the numbers refer to the cation valences), when plotted against the ratio of $\langle \text{oct-O} \rangle$ and $\langle \text{tet-O} \rangle$, are known to follow distinct curves on which the data points for inverse and normal spinels are located in separate sections (see p. 3289 in ref. [22]). In the case of our 4-3 spinel, with $u \equiv x_{\text{N/O}} = 0.255$, the calculated data point lies close to the section of inverse spinels. The fraction of site occupation, however, could not be determined from the present XRD data. We also should note that

the preference of Al for the octahedral site may not always be obeyed, as the actual fraction of site occupation of a spinel sialon with fixed composition is likely to depend on pressure, temperature, and the processing history of the material.

We have already noted that the determined lattice constant a_0 of $\gamma\text{-Si}_2\text{AlON}_3$ is 0.085 Å larger than that of $\gamma\text{-Si}_3\text{N}_4$ (Table 3). A linear increase of a_0 with increasing AlO content is well known for $\beta\text{-Si}_{3-x}\text{Al}_x\text{O}_x\text{N}_{4-x}$.^[9] Assuming a similar linear relation between lattice parameter and AlO content for $\gamma\text{-Si}_{3-x}\text{Al}_x\text{O}_x\text{N}_{4-x}$ ($0 \leq x \leq 3$), this correlation would extrapolate to the γ -alons $\text{Al}_{[3+(x-3)/3]}\text{O}_x\text{N}_{[1-(x-3)/3]}$ ($3 \leq x \leq 6$) if $\gamma\text{-Al}_3\text{O}_3\text{N}$ were to exist. Since stoichiometric $\gamma\text{-Al}_3\text{O}_3\text{N}$ has never been reported,^[6] we tried to estimate its lattice constant using data from three independent sources (Figure 2A): i) extrapolation of the two data points $a_0(x=1)$ [$\gamma\text{-Si}_2\text{AlON}_3$] from this work and $a_0(x=0)$ [$\gamma\text{-Si}_3\text{N}_4$] from ref. [8] yielded a value of 7.994 Å for $a_0(x=3)$; ii) extrapolation of the lattice constants of three Al_2O_3 -rich γ -alons investigated by Willems et al. using neutron diffraction^[12] yielded a value of about 7.980 Å; and iii) extrapolation of the lattice parameters of spinels in the Mg–Al–O–N system yielded a value of 7.986 Å.^[16] Thus, the three estimations give very similar results and support the hypothesis of a linear relation for $\gamma\text{-Si}_{3-x}\text{Al}_x\text{O}_x\text{N}_{4-x}$ (Figure 2A).

The compositional location of all nine data points within the reciprocal salt system $\text{SiO}_2\text{–Al}_2\text{O}_3\text{–AlN–Si}_3\text{N}_4$ is shown in Figure 2B. It is clear from Figure 2A that $\gamma\text{-Al}_3\text{O}_3\text{N}$ has a lower atomic density (ca. $9 \text{ Å}^3\text{atom}^{-1}$) than $\gamma\text{-Si}_3\text{N}_4$ ($8.27 \text{ Å}^3\text{atom}^{-1}$). The density of $\alpha\text{-Al}_2\text{O}_3$ is $8.49 \text{ Å}^3\text{atom}^{-1}$, and those of AlN are 8.35 and $8.27 \text{ Å}^3\text{atom}^{-1}$ for the low-^[17] and high-pressure^[18] modification, respectively. Only $\gamma\text{-Al}_2\text{O}_3$, with the defect spinel structure ($1/6$ sites empty), has a lower density ($9.3 \text{ Å}^3\text{atom}^{-1}$).^[19] Thus, according to Le Chatelier’s principle, on compression, $\gamma\text{-Al}_3\text{O}_3\text{N}$ should always be unstable with respect to decomposition into denser phases. This suggests that sialons of a sufficiently high AlO content cannot be converted to spinels under pressure.

Raman spectra with a spatial resolution of about 20 μm were taken from various parts of the $\gamma\text{-Si}_2\text{AlON}_3$ sample. All spectra were similar to that shown in Figure 3A showing broadened lines at 520, 830, 968, and 1020 cm^{-1} . Such line broadening and elevated background are most probably due to the submicrometer grain size and lattice defects. Similar results were observed for $\gamma\text{-Si}_3\text{N}_4$ synthesized^[8] in a multi-anvil apparatus.^[10a] In comparison, spectrum B in Figure 3 was taken from a $\gamma\text{-Si}_3\text{N}_4$ sample synthesized^[20] in a diamond-anvil cell.^[10a]

Table 3. Lattice parameters and relevant interatomic distances of different compositions in the $\gamma\text{-Si}_3\text{N}_4\text{–Alon–Al}_2\text{O}_3$ system.

	$\gamma\text{-Si}_3\text{N}_4$	$\gamma\text{-Si}_2\text{AlON}_3$	$\text{Al}_{3.35}\text{O}_{4.05}\text{N}_{0.65}$	$\text{Al}_{3.46}\text{O}_{4.38}\text{N}_{0.54}$	$\text{Al}_{3.54}\text{O}_{4.62}\text{N}_{0.46}$
Ref.	[8]	this work	[12]	[12]	[12]
a_0 [Å]	7.7381(2)	7.8234(3) ^[a]	7.9526(5)	7.9435(2)	7.9376(6)
$x_{\text{N/O}}$, $3m$	0.25968(1)	0.2550(4) ^[b]	0.2562(2)	0.2563(1)	0.2552(2)
$x_{\text{N/O}}$, $43m$	0.38468(1)	0.3800(4) ^[b]	0.3812(2)	0.3813(1)	0.3802(2)
$\langle \text{tet-N/O} \rangle$ [Å]	1.805	1.762	1.807	1.807	1.790
$\langle \text{oct-N/O} \rangle$ [Å]	1.863	1.918	1.940	1.937	1.944
$\langle \text{oct-N/O} \rangle / \langle \text{tet-N/O} \rangle$	1.032	1.089	1.073	1.072	1.086
$\langle \text{tet-oct} \rangle$ [Å]	3.208	3.243	3.297	3.293	3.291
$\langle \text{oct-oct} \rangle$ [Å]	2.737	2.766	2.812	2.808	2.806

[a] From data set I. [b] From data set II.

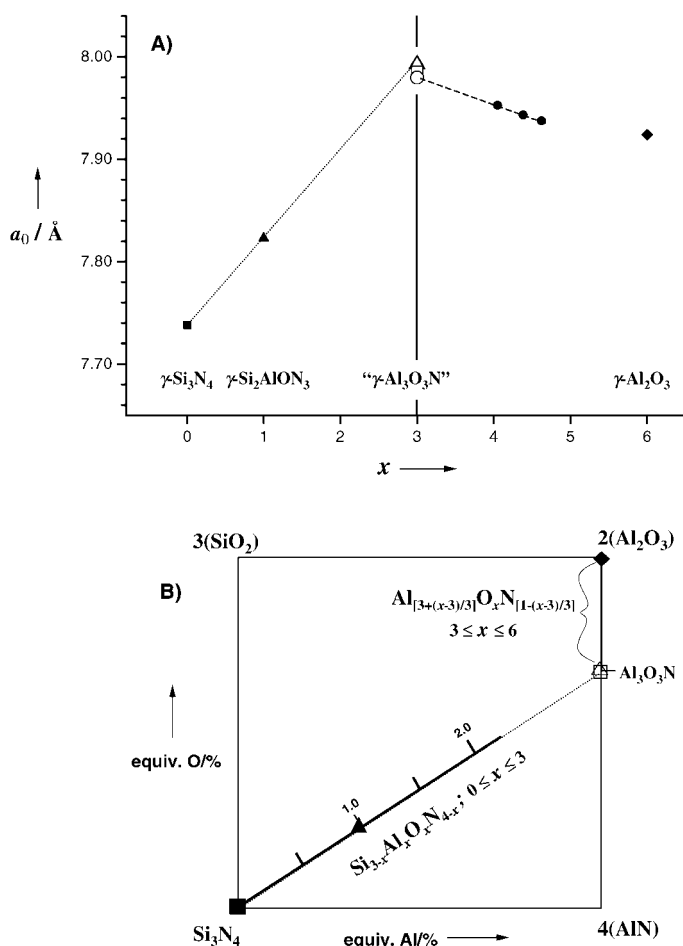


Figure 2. A) Lattice constants of different phases in the $\gamma\text{-Si}_3\text{N}_4\text{-alon-Al}_2\text{O}_3$ system. ■: ref. [8]; ▲: this work; △: extrapolated from ■ and ▲; □: ref. [16]; ●: ref. [12]; ○: extrapolated from ●; ◆: ref. [19]. B) Compositional location of data points in A) within the reciprocal salt system $\text{SiO}_2\text{-Al}_2\text{O}_3\text{-Si}_3\text{N}_4\text{-AlN}$.

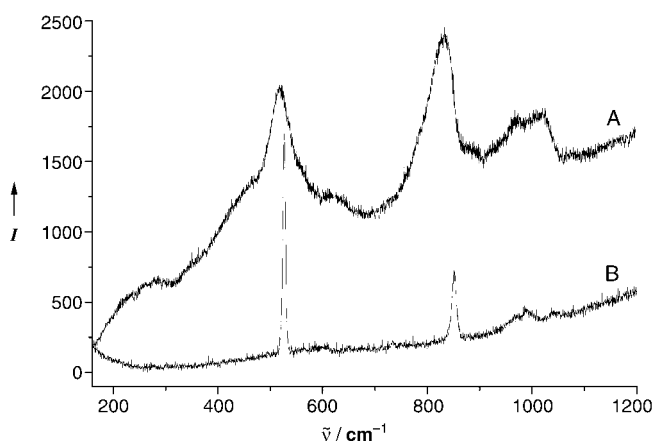


Figure 3. Raman spectra of the spinel nitrides $\gamma\text{-Si}_2\text{AlON}_3$ (A) and $\gamma\text{-Si}_3\text{N}_4$ (B). The spectrum of $\gamma\text{-Si}_2\text{AlON}_3$ (A) was measured at ambient pressure. The spectrum of $\gamma\text{-Si}_3\text{N}_4$ (B) was measured in a diamond-anvil cell at 1.1 GPa.

Here, the sharp bands indicate a well-crystallized material with a small amount of defects. This spectrum was obtained at 1.1 GPa, but the pressure dependence of the spectrum is small as the ambient-pressure frequencies are only 2–4 cm^{-1} lower

than those at 1.1 GPa.^[20] Comparing these Raman bands revealed a slight blue shift in the sialon sample, which may be due to the presence of Al and O ions within the spinel lattice.

Figure 4 shows an SEM image of Vickers indentations on the ground surface of $\gamma\text{-Si}_2\text{AlON}_3$. The quantities $2a$ and $2c$, used for determination of hardness and indentation fracture

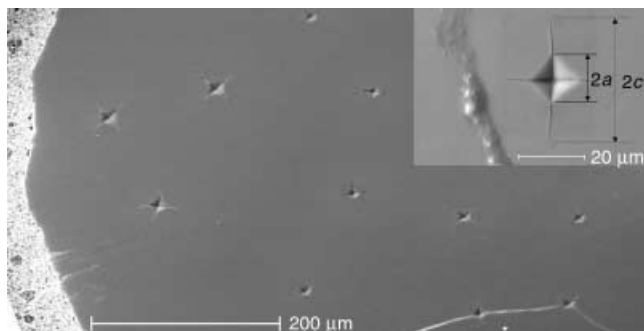


Figure 4. SEM image of $\gamma\text{-Si}_2\text{AlON}_3$ surface with $\text{HV}_{0.5}$ and HV_1 Vickers indentations and their radial crack systems. Inset: A $\text{HV}_{0.5}$ impression with indication of the indentation diagonal $2a$ and crack length $2c$.

toughness, are indicated. The average hardness from ten indentations at 0.5 kg ($\text{HV}_{0.5}$) and four indentations at 1.0 kg (HV_1) is as high as 2800 ± 60 (27.5 GPa). The HV_{10} values for the single-phase α - and β -sialons are usually 2200 and 1800, respectively,^[1, 9] and HV_{10} of γ -alon was also reported to be in the range of 1800.^[7] Therefore, γ -sialon appears to be a harder material. Since hardness is known to decrease with increasing applied load, future experiments on a larger specimen with a higher load (10 kg or more) would be desirable to confirm this observation.

Finally, a fracture toughness of $4.6 \text{ MPa m}^{1/2}$ was determined from the mean indentation crack length ($2c$). This is in the upper range of the toughness values for single-phase, fine-grain α - and β -sialons (typically 3–4.5 $\text{MPa m}^{1/2}$).^[1, 9]

Recently, it was shown that γ -sialons can also be synthesized by shock-compression techniques,^[21] which enable the preparation of larger amounts than the MA technique.^[10a] Also recently, we were able to synthesize γ -sialons with compositions $x = 1.1$, 2.0, and 2.1. Since spinel oxides encompass many desirable materials with magnetic, magnetoresistant, superconductive and other functional properties of technological relevance,^[22] the extension from spinel oxides to spinel oxide nitrides may hold great promise for the discovery of further novel and useful materials.

Experimental Section

Synthesis of β -sialon starting material: a powder mixture of 66.61 wt % Si_3N_4 (SN-E-10, Ube Industries, Japan, 1.32 wt % O), 11.40 wt % AlN (Type F, Tokuyama Soda Co., CA, 0.9 wt % O), and 21.99 wt % Al_2O_3 (AKP 50, Sumitomo Chemical America, NY) was prepared to give the nominal composition Si_2AlON_3 (the residual oxygen contents of the nitrides were taken into account). The powder was attrition-milled in isopropyl alcohol for 2 h with high-purity Si_3N_4 milling medium in a Teflon-coated jar. The slurry was dried in a polyethylene beaker under a halogen lamp while being stirred. Finally, charges of the powder were uniaxially hot-pressed (30 MPa) in a graphite furnace (1775 °C/2 h/ N_2). Phase analysis was performed by XRD with $\text{CuK}\alpha$ radiation and Si as an internal standard. The analysis showed mostly β -phase with a small amount (< 2%) of $\alpha\text{-Si}_3\text{N}_4$.

The lattice constant of the β -phase was in good agreement with the composition Si_2AlON_3 .^[9]

High-pressure synthesis of γ -sialon was performed in a 6-8 type multi-anvil (MA) apparatus. A detailed description of similar MA devices is given elsewhere.^[10]

A cylinder ($\varnothing = 1.45$; $h = 2.7$ mm; $m = 12.5$ mg) was cored out of a hot-pressed β -sialon compact, wrapped in a 25 μm thick Pt foil, and placed inside a set of coaxially arranged ceramic components (from inside to outside): MgO insulation, LaCrO₃ resistance heater, ZrO₂ tubing. The further pressure assembly was identical that in ref. [8]. The sample was brought to maximum pressure at about 25 °C, heated to 1800 °C at about 100 K min⁻¹, and then immediately quenched to room temperature in less than 15 s. Temperatures were measured with W₇₇Re₃–W₇₅Re₂₅ thermocouples. For details on temperature measurement and pressure calibration see ref. [10b,c].

Surface preparation: The obtained γ -sialon and a piece of the β -sialon phase were embedded in a glass-fiber-filled diallylphthalate matrix (Resin 5, Struers) and wet ground down to 4000 mesh SiC paper to give a surface suitable for indentation measurements. For SEM and EPMA, the sample was sputtered with a ca. 10-nm film of carbon.

HR-SEM was performed on a Philips XL30 FEG with a lateral resolution of 1 nm.

EPMA: Cameca SX-50. Measurements at 20 kV and 20 nA for all elements. Mappings at 20 kV, 49 nA, beam-scan mode, 256 × 256 data points, step size ~0.4 μm . Detectors: TAP for Al, 30 s/data point; PET for Si, 30 s/data point; and PC1 for N and O, 60 s/data point for each element.

X-ray powder diffractometry: Data set I was obtained from the quartz-contaminated γ -sialon, measured in transmission geometry on a Stoe STADI-P diffractometer equipped with a position-sensitive detector covering 6°. The diffractogram of the pure material (data set II, Figure 1) was obtained as follows: A piece of γ -Si₂AlON₃ (70 μm in diameter, ca. 20 μm thick) was split from the central portion of the cylindrical sample. It was mounted on a capillary in a Gandolfi camera. By using a fine-focus rotating anode (GX21, Enraf-Nonius), a two-dimensional diffraction pattern was detected with a flat imaging plate (23 × 25 cm) positioned at a distance of 119 mm from the sample. It was read out with a spatial resolution of 50 μm with an imaging analyzer (BAS-1800II, Fuji Film). To obtain a standard one-dimensional diffraction pattern (data set II), the intensities were integrated along the azimuthal direction.

Rietveld refinement was carried out with the program LHPM-7^[23] and the scattering curves of neutral atoms were used, since Si⁴⁺, Al³⁺, O²⁻, and N³⁻ scattering curves lead to nearly the same result. Also, no significant difference could be seen on positioning Al at 8a and Si at 16d, or vice versa. The temperature parameters of the 16d and 32e site were treated anisotropically.

Micro-Raman spectroscopy: Ar-ion laser ($\lambda = 457.9$ nm, 2020-05S, Spectra-Physics, San Jose, CA); double spectrometer (SPEX 1402, Spex Industries, Metuchen, NJ) with a charge coupled device detector (LN/CCD-1100 FB, Princeton Instruments, Trenton, NJ, lateral resolution ~20 μm).

Vickers hardness measurements were made under ambient atmosphere with a LECO M-400 G2 hardness tester. Each hardness value HV was calculated according to equation (1) where P is the load in kilograms, $\phi = 136^\circ$ the apex angle of the Vickers pyramid, and $(2a)$ the mean indentation diagonal (Figure 4).^[24] A mean HV_{0.5} value of 2789 ± 64 was obtained from ten indentations at a load of 0.5 kg, and four further indentations with a 1-kg load (HV₁) gave 2838 ± 32 ; this led to an overall mean Vickers hardness of 2808 ± 60 (ca. 27.5 GPa). The peak load was applied for 10 s in all cases.

$$\text{HV} = P2 \sin(\phi/2) / (2a)^2 \quad (1)$$

Indentation fracture toughness (K_{IC} -IF) was determined by assuming a Palmquist crack geometry; because of its good correlation to bending-test derived data, the formula given by Shetty was chosen.^[25] A mean K_{IC} -IF of 4.6 MPa m^{1/2} was calculated from four of the 0.5-kg and three of the 1-kg indentations, by using the mean crack lengths $(2c)$ and indentation diagonals $(2a)$ obtained for each indentation and the respective hardness values in SI units. The ratio $\langle c \rangle / \langle a \rangle$ varied between 2.5 and 3.2 for all indentations.

Received: September 20, 2001 [Z17937]

- [1] T. Ekström, M. Nygren, *J. Am. Ceram. Soc.* **1992**, 75, 259–276.
- [2] a) J.-W. Chen, R. Shulua in *Encyclopedia of Materials: Science and Technology* (Eds.: K. H. J. Buschow, R. W. Cahn, M. C. Flemmings, B. J. Schermer, E. J. Kramer, S. Mahajan), Elsevier, Amsterdam, **2001**, pp. 8471–8476; b) F. L. Riley, *J. Am. Ceram. Soc.* **2000**, 83, 246–265.
- [3] a) M. Haviar, H. Herbertsson, *J. Mater. Sci. Lett.* **1992**, 11, 179–180; b) M. Haviar, H. Herbertsson, *J. Mater. Sci. Lett.* **1993**, 12, 1888–1890; c) M. Haviar, Z. Lences, H. Herbertsson, *J. Mater. Sci. Lett.* **1997**, 16, 236–238.
- [4] a) A. Zerr, G. Miehe, G. Serghiou, M. Schwarz, E. Kroke, R. Riedel, H. Fueß, P. Kroll, R. Boehler, *Nature* **1999**, 400, 340–342; b) G. Serghiou, G. Miehe, O. Tschauner, A. Zerr, R. Boehler, *J. Chem. Phys.* **1999**, 111, 4659–4661; c) K. Leinenweber, P. F. McMillan, G. H. Wolf, *Chem. Eur. J.* **1999**, 5, 3076–3078; d) N. Scotti, W. Kockelmann, J. Senker, S. Traßel, H. Jacobs, *Z. Anorg. Allg. Chem.* **1999**, 625, 1435–1439.
- [5] Often the formula Si_{6–z}Al_zO_{8–z}N_z is used, but here we follow the recommendation of Ekström and Nygren^[1] for a nomenclature that indicates the Si₃N₄ parent phase more clearly.
- [6] a) J. W. McCauley, personal communication; b) “ γ -Al₃O₃N” is found in the JCPDS database (PDF-No. 36-50). However, in the respective publication (W. Rafaniello, I. B. Cutler, *J. Am. Ceram. Soc.* **1981**, C128) no information on the composition of the products is given.
- [7] a) J. W. McCauley, N. D. Corbin, *NATO ASI Ser. Ser. E* **1983**, 65, 111–118; b) J. W. McCauley, N. D. Corbin, *J. Am. Ceram. Soc.* **1979**, 63, 9–10; J. W. McCauley, N. D. Corbin, *J. Am. Ceram. Soc.* **1979**, 63, 467–469.
- [8] M. Schwarz, G. Miehe, A. Zerr, E. Kroke, B. T. Poe, H. Fueß, R. Riedel, *Adv. Mater.* **2000**, 12, 883–887.
- [9] T. Ekström, P. O. Käll, M. Nygren, P. O. Olsson, *J. Mater. Sci. Lett.* **1989**, 24, 1853–1861.
- [10] a) For an overview, see: E. Kroke, *Angew. Chem.* **2002**, 114, 81–86; *Angew. Chem. Int. Ed.* **2002**, 41, 77–82; b) D. C. Rubie, *Phase Transitions* **1999**, 68, 431–451; c) M. J. Walter, Y. Thibault, K. Wei, R. W. Luth, *Can. J. Phys.* **1995**, 73, 273–286.
- [11] Value given with respect to the unit cell origin at $\bar{3}m$.
- [12] H. X. Willems, G. de With, R. Metselaar, R. B. Helmholtz, K. K. Petersen, *J. Mater. Sci. Lett.* **1993**, 12, 1470–1473.
- [13] K. E. Sickafus, J. M. Wills, *J. Am. Ceram. Soc.* **1999**, 82, 3279–3292.
- [14] Individual unit cells within Si_{3–x}Al_xO_{8–x}N_{4–x} in which x is nonintegral would not have identical Si:Al ratios, even for a nonrandom distribution. Consequently, individual Si–O, Si–N, Al–O, and Al–N bond lengths will show slight deviations from a mean cation–anion bond length. This is indicated by the angle brackets $\langle \rangle$ and \rangle .
- [15] a) K. Kato, Z. Inoue, K. Kijima, I. Kawada, H. Tanaka, T. Ymane, *J. Am. Ceram. Soc.* **1975**, 58, 90–91; b) R. Grün, *Acta Crystallogr.* **1979**, 35, 800–804.
- [16] J. Weiss, P. Greil, L. J. Gauckler, *J. Am. Ceram. Soc.* **1982**, C68–C69. (A value of a_0 for Al₃O₃N is not given explicitly, but can be obtained by extrapolation to the ordinate, as indicated in Figure 2 on p. C68.)
- [17] H. Schulz, K. Thiemann, *Solid State Commun.* **1977**, 23, 815–819.
- [18] H. Vollstädt, E. Ito, M. Akaishi, S. Akimoto, O. Fukunaga, *Proc. Jpn. Acad. Ser. B* **1990**, 66, 7–9.
- [19] JCPDS Database, PDF-No. 10-425.
- [20] A. Zerr, G. Miehe, G. Serghiou, M. Schwarz, E. Kroke, R. Riedel, R. Boehler, *Science and Technology of High Pressure* (Eds.: M. Manghnani, W. J. Nellis, M. F. Nicol), Universities Press, Hyderabad, India, **2000**, pp. 914–917.
- [21] T. Sekine, H. He, T. Kobayashi, M. Tansho, K. Kimoto, *Chem. Phys. Lett.* **2001**, 344, 395–399.
- [22] “Spinel Compounds: Structure and Properties Relations”: *J. Am. Ceram. Soc.* **1999**, 82, 3279–3365 (topical issue).
- [23] a) D. B. Wiles, R. A. Young, *J. Appl. Crystallogr.* **1981**, 14, 149–151; b) R. J. Hill, C. J. Howard, Australian Atomic Energy Commission, Report No M112, **1986**.
- [24] *Werkstoffprüfung*, 5th ed. (Ed.: H. Blumenauer), VEB Deutscher Verlag für Grundstoffindustrie, Leipzig, **1984**, pp. 118–119.
- [25] J. Dusza, *Scr. Metall. Mater.* **1992**, 26, 337–342.